Article

Switching the Redox Mechanism: Models for Proton-Coupled Electron Transfer from Tyrosine and Tryptophan

Martin Sjdin, Stenbjrn Styring, Henriette Wolpher, Yunhua Xu, Licheng Sun, and Leif Hammarstrm

J. Am. Chem. Soc., **2005**, 127 (11), 3855-3863• DOI: 10.1021/ja044395o • Publication Date (Web): 25 February 2005

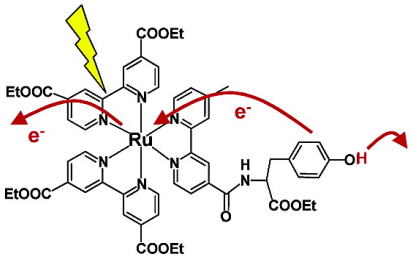

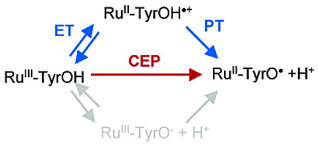

More About This Article

Additional resources and features associated with this article are available within the HTML version:

- Supporting Information
- Links to the 28 articles that cite this article, as of the time of this article download
- Access to high resolution figures
- Links to articles and content related to this article
- Copyright permission to reproduce figures and/or text from this article

View the Full Text HTML

J|A|C|S
ARTICLES
Published on Web 02/25/2005

Switching the Redox Mechanism: Models for Proton-Coupled Electron Transfer from Tyrosine and Tryptophan

Martin Sjödin,[†] Stenbjörn Styring,[‡] Henriette Wolpher,[§] Yunhua Xu,[§] Licheng Sun,[§] and Leif Hammarström*[,†]

Contribution from the Department of Physical Chemistry, BMC, Uppsala University, P.O. Box 579, SE-751 23 Uppsala, Sweden, Department of Molecular Biomimetics, Uppsala University, Villavägen 6, SE-752 36 Uppsala, Sweden, and Department of Organic Chemistry, Arrhenius Laboratories, Stockholm University, SE-106 91 Stockholm, Sweden

Received September 15, 2004; E-mail: Leifh@fki.uu.se

Abstract: The coupling of electron and proton transfer is an important controlling factor in radical proteins, such as photosystem II, ribinucleotide reductase, cytochrome oxidases, and DNA photolyase. This was investigated in model complexes in which a tyrosine or tryptophan residue was oxidized by a laser-flash generated trisbipyridine−Ru^{III} moiety in an intramolecular, proton-coupled electron transfer (PCET) reaction. The PCET was found to proceed in a competition between a stepwise reaction, in which electron transfer is followed by deprotonation of the amino acid radical (ETPT), and a concerted reaction, in which both the electron and proton are transferred in a single reaction step (CEP). Moreover, we found that we could analyze the kinetic data for PCET by Marcus' theory for electron transfer. By altering the solution pH, the strength of the Ru^{III} oxidant, or the identity of the amino acid, we could induce a switch between the two mechanisms and obtain quantitative data for the parameters that control which one will dominate. The characteristic pH-dependence of the CEP rate (M. Sjödin et al. *J. Am. Chem. Soc.* **2000**, *122*, 3932) reflects the pH-dependence of the driving force caused by proton release to the bulk. For the pH-independent ETPT on the other hand, the driving force of the rate-determining ET step is pH-independent and smaller. On the other hand, temperature-dependent data showed that the reorganization energy was higher for CEP, while the pre-exponential factors showed no significant difference between the mechanisms. Thus, the opposing effect of the differences in driving force and reorganization energy determines which of the mechanisms will dominate. Our results show that a concerted mechanism is in general quite likely and provides a low-barrier reaction pathway for weakly exoergonic reactions. In addition, the kinetic isotope effect was much higher for CEP ($k_H/k_D > 10$) than for ETPT ($k_H/k_D = 2$), consistent with significant changes along the proton reaction coordinate in the rate-determining step of CEP.

Introduction

Amino acid radicals are key intermediates in many enzymatic redox reactions.[1] Electron transfer from an amino acid is often coupled to deprotonation. The two reactions may occur one before the other in a stepwise mechanism, or in a single, concerted step. These alternatives give widely different reaction properties. Because proton-coupled electron transfer (PCET) controls electron and proton flow in the proteins, and is important for catalytic substrate reactions, these mechanisms are intensely debated. Important examples include photosystem II,[2] DNA photolyase,[3] cytochrome oxidases,[4] and ribonucleotide reductase (RNR).[5] Marcus theory[6] and results from model systems[7] have been instrumental for the understanding of single electron transfer in proteins,[8] and these tools need to be extended to include PCET. Here we present new experimental data for PCET from tyrosine and tryptophan in model complexes.

We have previously demonstrated that intramolecular oxidation of tyrosine by Ru^{III} in a covalently linked complex (Ru−Tyr_{ref},[9] Figure 1a) is concerted with tyrosine deprotonation.[10] This is in contrast to frequent belief that a concerted transfer is in general an improbable event. The Ru−Tyr_{ref} differs from previous model systems for PCET[11,12] in that the electron and proton are transferred in different directions, a situation found in, e.g., photosystem II and RNR. Furthermore, the reaction driving force ($-\Delta G^{\circ\prime}$) is pH-dependent because the proton is released

[†] Department of Physical Chemistry, BMC, Uppsala University.
[‡] Department of Molecular Biomimetics, Uppsala University.
[§] Stockholm University.

(1) Stubbe, J.; van der Donk, W. *Chem. Rev.* **1998**, *98*, 705.
(2) Hoganson, C. W.; Babcock, G. T. *Science* **1997**, *277*, 1953.
(3) Aubert, C.; Vos, M. H.; Mathis, P.; Eker, A. P. M.; Brettel, K. *Nature* **2000**, *405*, 586.
(4) Babcock, G. T. *Proc. Natl. Acad. Sci. U.S.A.* **1999**, *96*, 12971.
(5) Stubbe, J.; Nocera, D. G.; Yee, C. S.; Chang, M. C. Y. *Chem. Rev.* **2003**, *103*, 2167.
(6) Marcus, R. A.; Sutin, N. *Biochim. Biophys. Acta* **1985**, *811*, 265.
(7) (a) Closs, G. L.; Miller, J. R. *Science* **1988**, *240*, 440. (b) Balzani, V., Ed.; *Electron Transfer in Chemistry*; WILEY-VCH: Wienheim, 2001; Vol. 3.
(8) (a) Gray, H. B.; Winkler, J. R. *Annu. Rev. Biochem.* **1996**, *65*, 537. (b) Page, C. C. Moser, C. C.; Chen, X.; Dutton, P. L. *Nature* **1999**, *402*, 47.
(9) Magnuson, A.; Berglund, H.; Korall, P.; Hammarström, L.; Åkermark, B.; Styring, S.; Sun. L. *J. Am. Chem. Soc.* **1997**, *119*, 10720.
(10) Sjödin, M.; Styring, S.; Åkermark, B.; Sun, S.; Hammarström, L. *J. Am. Chem. Soc.* **2000**, *122*, 3932.

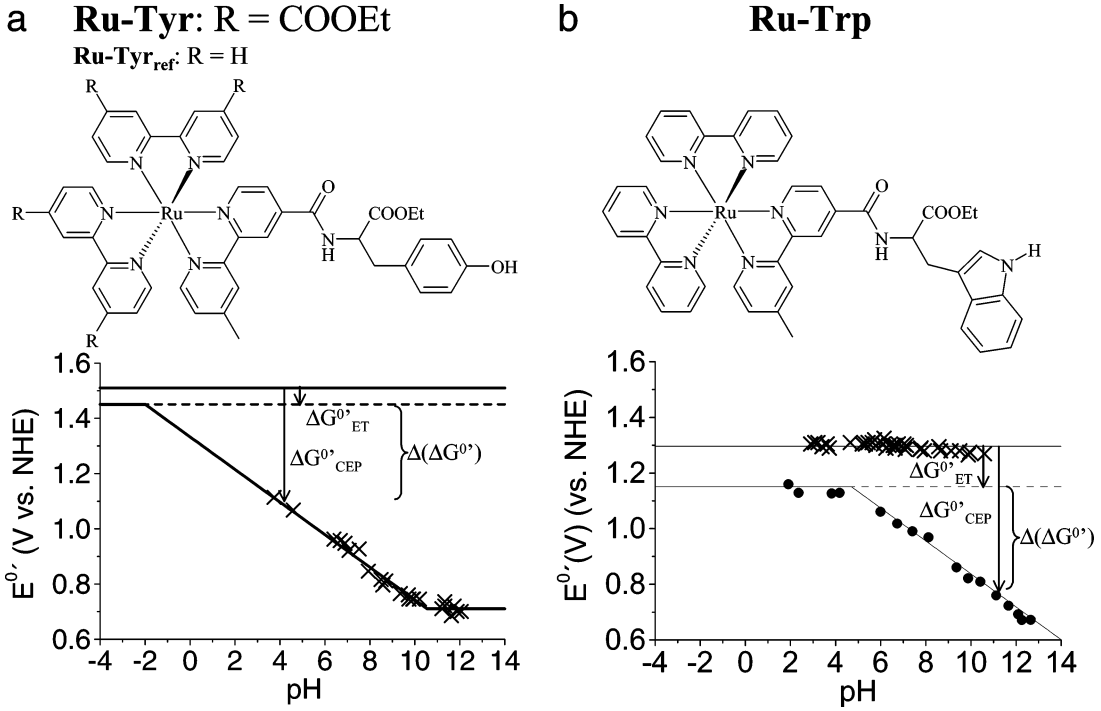

Figure 1. Structure and electrochemical potentials of **Ru-Tyr** and **Ru-Trp**. (a) The potential (DPV peak potentials) for oxidation of the tyrosine moiety in **Ru-Tyr** (crosses). The line is the theoretically expected pH-dependence of the potential (see text). The $Ru^{III/II}$ potential is calculated from data in acetonitrile (solid line at $E^{o\prime} = 1.53$ V). (b) The potential (DPV peak potentials) for oxidation of the tryptophan moiety (dots) and the $Ru^{III/II}$ potential (crosses) in **Ru-Trp**. The driving force for CEP ($-\Delta G^{o\prime}_{CEP}$) is given by the difference between the $Ru^{III/II}$ and $Tyr^{\bullet}$/TyrH (or $Trp^{\bullet}$/TrpH) potentials, while that for the ET step of ETPT ($-\Delta G^{o\prime}_{ET}$) is given by the difference between the $Ru^{III/II}$ and $TyrH^{\bullet+}$/TyrH (or $TrpH^{\bullet+}$/TrpH) potentials (see text).

to bulk water. The rate constant dependence on pH was found to follow Marcus' equation[6] for pure electron transfer, with the pH-dependent $-\Delta G^{\circ\prime}$ as the free energy parameter. This behavior and analysis had not previously been reported for PCET.[11,12] Moreover, our comparison with data for $Tyrosine_Z$ oxidation in manganese-depleted photosystem II suggested that also this reaction at pH < 7 is concerted with proton release to the bulk.

Concerted and stepwise PCET show very different reaction characteristics. The concerted reaction is "energy conservative" in that it avoids charged intermediates in a low-dielectric environment such as a protein. On the other hand, our data revealed that the reorganization energy is large, which may give a slow, highly activated reaction.[13,14] The competition between concerted and stepwise PCET may thus be governed by the opposing effects of more favorable energetics and a larger reorganization energy for the concerted mechanism. To investigate this competition quantitatively, we have in this report modified our $Ru-Tyr_{ref}$ model system by either increasing the potential of the ruthenium oxidant with ethylester substituents on the bipyridine ligands (**Ru-Tyr**) or by replacing the tyrosine with a tryptophan residue (**Ru-Trp**); see Figure 1. Both modifications alter the energetics for PCET, so that we are able to demonstrate a switch between a concerted and a stepwise mechanism in the same complex.[15] Based on a Marcus model we thus obtain quantitative data for the parameters controlling the two different mechanisms, which should be useful to understand radical protein reactions.

Experimental Section

Ru-Tyr was available from a previous study.[16] **Ru-Trp** was synthesized by reacting the functionalized Ru(bpy)2(4-methyl-4′-COCl-bpy) precursor[16] with L-tryptophan ethyl ester in the presence of triethylamine, followed by column chromatography on silica gel. The structure was confirmed by NMR and ESI-MS.

Differential pulse voltammetry measurements of **Ru-Tyr** and **Ru-Trp** were made in buffered water solution with 0.5 M KCl (MERCK, p.a. grade) as electrolyte. Na_2HPO_4 (SigmaUltra, 99%), 10 mM, and H_3BO_3 (Sigma, 99.5%), 10 mM, were used as buffers. For **Ru-Trp** the analyte concentration was 0.5 mM, and for Ru-Tyr a saturated solution (~0.2 mM) was used due to the lower solubility of **Ru-Tyr** in water. The solution pH was adjusted with HCl_{aq} or $NaOH_{aq}$ and measured directly in the cell prior to and after every measurement. Before all measurements oxygen was removed by bubbling the stirred solution with solvent-saturated argon, and the samples were kept under argon atmosphere during measurements.

(11) In other studies of tyrosine or phenol oxidation, the pH-dependent reactivity of the acid (phenol) form has probably been masked by the interference from the more reactive base (phenolate) form. In our studies, the *intramolecular* reactions of these two species with Ru^{III} can be studied separately, giving biphasic kinetics around the tyrosine pK_a. In addition, previous studies of PCET have concerned very different aspects and analyses; see, e.g., ref 12.

(12) (a) Cukier, R. I.; Nocera, D. *Annu. Rev. Phys. Chem.* **1998**, *49*, 337. (b) Cukier, R. I. *J. Phys. Chem. B* **2002**, *106*, 1746. (c) Roth, J. P.; Yoder, J. C.; Won, T.-J.; Mayer, J. M. *Science* **2001**, *294*, 2524. (d) Hammes-Schiffer, S. *Acc. Chem. Res.* **2001**, *34*, 273.

(13) Quantum mechanical calculations on the model complex in ref 10 were recently presented in ref 14. The authors discuss effects that cannot be accounted for in our semiclassical analysis based on experimental data, and although the agreements dominate, these authors have a somewhat different opinion from ours.

(14) Carra, C.; Iordanova, N.; Hammes-Schiffer, S. *J. Am. Chem. Soc.* **2003**, *125*, 10429.

(15) (a) We have recently demonstrated qualitatively that we could switch the mechanism of PCET in a modified Ru−Tyr complex, although protonable groups on the Ru moiety complicated the situation and precluded a quantitative analysis; see ref 15b. (b) Sjödin, M.; Ghanem, R.; Polivka, T.; Pan, J.; Styring, S.; Sun, L.; Sundström, V.; Hammarström, L. *Phys. Chem. Chem. Phys.* **2004**, *6*, 4851.

(16) Ghanem, R.; Xu, Y.; Pan, J.; Hoffman, T.; Andersson, J.; Polivka, T.; Pascher, T.; Styring, S.; Sun, L.; Sundström, V. *Inorg. Chem.* **2002**, *41*, 6258.

For the electrochemical measurements a three-electrode system connected to an Eco Chemie model Autolab/GPES electrochemical interface was used. The reference electrode, Ag/AgCl in saturated KCl, was calibrated versus methyl viologen using the same experimental conditions as for the sample. A glassy carbon electrode was used as counter electrode. Both reference and counter electrodes were separated from the sample solution by porous glass membranes. The working electrode was a 2-mm diameter glassy carbon electrode. Before every measurement the working electrode was thoroughly polished with 0.3-μm aluminum oxide (BDH Laboratory Supplies) to remove deposited products from previous measurements.

Laser flash photolysis with transient absorption detection was used to investigate the electron-transfer reactions occurring in **Ru-Tyr** and **Ru-Trp**. In these experiments the analyte, **Ru-Tyr** or **Ru-Trp**, and methyl viologen dichloride, MV^{2+} (Sigma-Aldrich), or hexaaminеruthenium(III), $[Ru(NH_3)_6]^{3+}$ (Aldrich, 98%), was dissolved in buffered water solution to a concentration of 40−60 μM and 200 mM, respectively. As in the electrochemical experiments the buffer was 10 mM Na_2HPO_4 (SigmaUltra, 99%) and 10 mM H_3BO_3 (Sigma, 99.5%), the pH was adjusted with HCl_{aq} or $NaOH_{aq}$ before dissolving the analyte, and the sample solution was purged with argon prior to measurements and kept under argon atmosphere during measurements. As a control lower buffer concentrations, 1 mM Na_2HPO_4 and 1 mM H_3BO_3, were used at some selected pH values. To determine the deuterium isotope effect deuterium oxide (Aldrich 99.9% D) was used as solvent, all other conditions being the same as in the water experiments.

The intramolecular electron transfer from the amino acid residue to the $[Ru(bpy)_3]^{3+}$ moiety of **Ru-Tyr** or **Ru-Trp** was investigated using a flash-quench method described earlier.[9,10] The $[Ru(bpy)_3]^{2+}$ unit was excited with a 5-ns 460-nm laser pulse (ca. 20 mJ/pulse on a 0.4-cm^2 spot), and the excited state was oxidatively quenched by methyl viologen MV^{2+} or $[Ru(NH_3)_6]^{3+}$ giving the Ru^{III} complex of **Ru-Tyr** or **Ru-Trp**. The subsequent electron transfer from the amino acid to Ru^{III} was followed by the recovery of the Ru^{II} ground-state signal at 450 nm. Recombination between $MV^{\bullet+}$ and $[Ru(bpy)_3]^{3+}$ or the amino acid radical could be controlled by monitoring the disappearance of the $MV^{\bullet+}$-absorption at 600 nm. In all measurements this recombination reaction was very slow compared to the intramolecular electron transfer and therefore neglected in the kinetic analysis. The first-order rate constant for the electron transfer between Ru^{III} and amino acid was determined by fitting the 450 nm transients to a single-exponential function. Each transient curve was an average of 16 individual laser shots. The rate constants reported at different pH values and temperatures are in turn averages from an analysis from at least six curves recorded under identical conditions. For **Ru-Tyr** the variance of the extracted rate constants was about 5% of the absolute rate constant. The corresponding value for **Ru-Trp** was about 20%. In all measurements the temperature was kept at 298 K using a Hetrofrig thermostat if not stated otherwise.

Analyzing light was produced by a pulsed Xenon lamp, and after passing the sample at a right angle relative to the laser pulse, the light was detected as a function of time with a Hamamatsu R928 photomultiplier.

Results and Discussion

Electrochemical Potentials. The driving force for PCET in **Ru-Tyr** and **Ru-Trp** is given by the difference in redox potential for the $Ru^{III/II}$ couple and the $Tyr^{ox/red}$ and $Trp^{ox/red}$ couples, respectively. Figure 1 shows these potentials as a function of pH. The tyrosine potential in **Ru-Tyr** was determined by differential-pulse voltammetry and is in good agreement with previous reports for tyrosine.[17] The pK_a value of the reduced tyrosine form was determined to 10.3 from the breaking point between the pH-dependent and pH-independent regions. The pH-dependence of the $Ru(bpy)_3^{2+}$-based emission quenching gave the same pK_a value.[18] At pH < 10 the potential shows a pH-dependence consistent with the expected 59 mV/pH unit for a one proton/one electron couple. Below the pK_a value of the oxidized form (p$K_a = -2$[19]), the potential should become pH-independent again, although this was not possible to verify experimentally.

The tryptophan potential in **Ru-Trp** was determined in the same way, but at some pH regions we observed a two-electron oxidation (see Supporting Information) that is not relevant for the light-induced one-electron reactions below. Two-electron electrochemical oxidation of tryptophan and other indoles has previously been reported and attributed to rapid further oxidation of the initial product.[20] Instead, we plot the data for one-electron oxidation of tryptophan from ref 17a in Figure 1. This shows a pH-independent potential below the pK_a of the oxidized tryptophan (4.7)[21] and a 59 mV/pH unit decrease as pH increases above that value. The tryptophan has a p$K_a \approx 17$[22] before oxidation, so this deprotonation is not seen in the accessible pH range. Our own data in the pH-independent region (pH < 4.7), $E_{peak} = 1.13$ V vs NHE, is in good agreement with that reported in ref 17a.

The ruthenium potential in **Ru-Trp** was ca. 1.29 V vs NHE, independent of pH (Figure 1a), as expected for a $Ru(bpy)_3^{2+}$ complex.[23] The <40 mV apparent variation over 8 pH units can be ascribed to the uncertainty in subtraction of the pH-dependent background current for water oxidation at this high potential range. In **Ru-Tyr** the ruthenium potential is much higher due to the electron-withdrawing ester substituents, and the oxidation could not be resolved from the water-oxidation background current. Instead we make the reasonable assumption that the difference in ruthenium potential between **Ru-Tyr** and **Ru-Trp** is the same in aqueous and acetonitrile solution. Ruthenium potential values of 1.14 V (vs ferrocenium/ferrocene) for **Ru-Tyr** and 0.90 V for **Ru-Trp** were measured in acetonitrile, giving a potential difference of 0.24 V. Thus, by adding 0.24 V to the aqueous potential for **Ru-Trp** above, a value of 1.53 V vs NHE for **Ru-Tyr** in water is obtained and is drawn as a solid line in Figure 1b.

Light-Induced PCET. The PCET from the tyrosine or tryptophan moieties to the oxidized Ru^{III} (eq 1) in **Ru-Tyr** and **Ru-Trp** was triggered by the "flash-quench method".[9,10,24] About 50 μM complex was dissolved in 0.01 M phosphate/borate buffer, and 0.2 M electron acceptor methyl viologen or hexaaminеruthenium(III) was added. A ca. 5-ns laser flash at 460 nm excited the Ru^{II} moiety that was rapidly (τ < 10 ns) oxidized to Ru^{III} by the external electron acceptor (eq 1):

$$[Ru^{II}-TyrH]^{2+} + MV^{2+} + h\nu \rightarrow [{}^*Ru^{II}-TyrH]^{2+} + MV^{2+} \rightarrow [Ru^{III}-TyrH]^{3+} + MV^{\bullet+} \quad (1a)$$

$$[Ru^{II}-TrpH]^{2+} + MV^{2+} + h\nu \rightarrow [{}^*Ru^{II}-TrpH]^{2+} + MV^{2+} \rightarrow [Ru^{III}-TrpH]^{3+} + MV^{\bullet+} \quad (1b)$$

This was seen from the rapid appearance of the $MV^{\bullet+}$ absorption

(17) (a) Harriman, A. *J. Phys. Chem.* **1987**, *91*, 6102. (b) Tommos, C.; Skalicky, J. J.; Pilloud, D. L.; Wand, A. J.; Dutton, P. L. *Biochemistry* **1999**, *38*, 9495.

(18) The **Ru-Tyr** in the protonated tyrosine form showed an unquenched emission lifetime of ca. 400 ns, while the emission lifetime for the tyrosinate form of the complex was only ca. 40 ns. Around the pK_a value the emission decay was biexponential, and at pH = 10.3 the amplitudes of the two kinetic components were equal. Note that the protonation state did not change on the timescale of the excited state lifetime, as shown by the pH-independence of the component lifetimes.

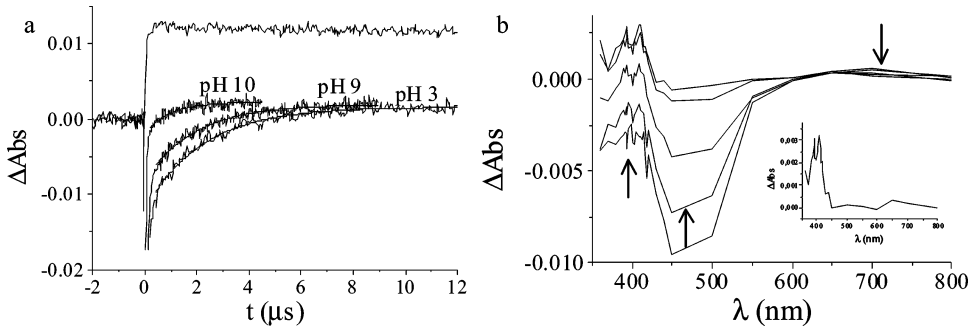

Figure 2. (a) Transient absorbance traces for **Ru-Tyr** (ca. 50 μM) after a 460 nm laser flash in the presence of 0.2 M methyl viologen (MV^{2+}), showing the rapid generation of the $MV^{\bullet+}$ radical at 600 nm (upper trace) and Ru^{II} ground-state bleach at 450 nm (lower traces). The recovery of the 450 nm bleach monitors the subsequent intramolecular PCET from the tyrosine unit to the Ru^{III} and shows pH-dependent kinetics. The lower amplitude at pH = 10 is because a large fraction of the tyrosine is already deprotonated and reacts with Ru^{III} much faster. The traces at 600 nm were not pH-dependent. (b) Transient absorption spectra at 0.7, 1.2, 2.2, 4.6, and 7.2 μs after the laser flash for the same type of experiment as in that part a, but with 0.2 M hexaminеruthenium-(III) as acceptor instead of MV^{2+}. The initial broad bleach around 450 nm, due to formation of Ru^{III}, disappears and with the same kinetics a spectrum characteristic of the deprotonated tyrosine radical appears,[28] with maxima around 410 nm and a broad band at 600−750 nm. (Inset) The transient spectrum after 7.8 μs with the ~3% residual Ru^{II} bleach subtracted (see text), showing the tyrosine radical spectrum.

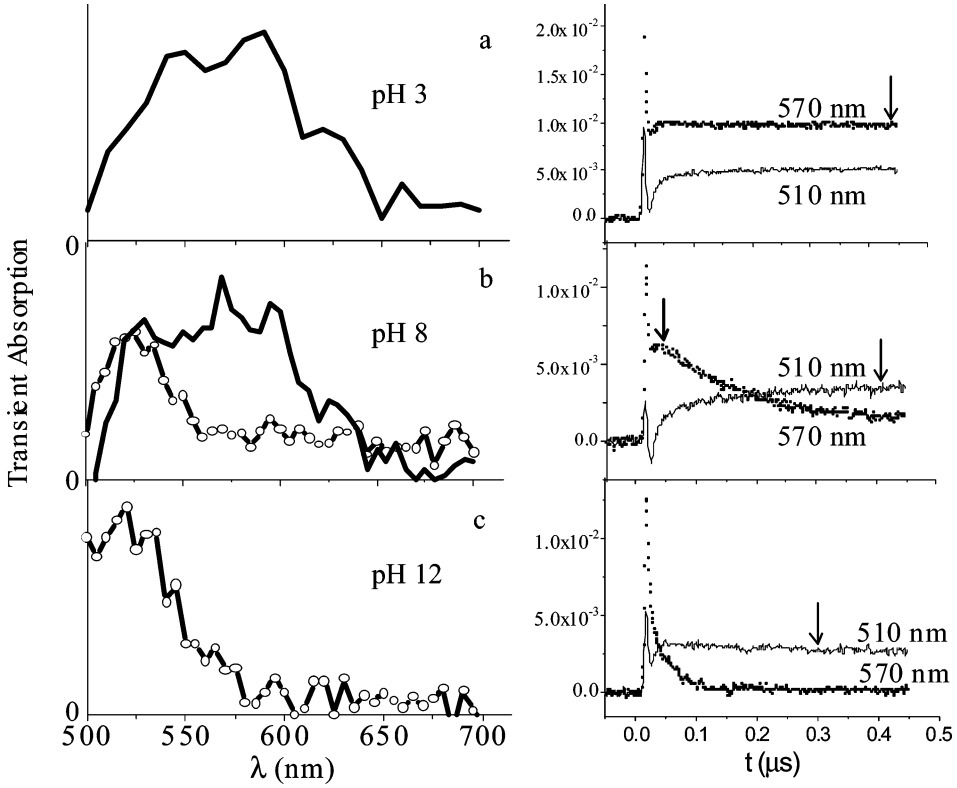

Figure 3. Transient absorption spectra of **Ru-Trp** (ca. 50 μM) after electron transfer from the tryptophan to the flash-quench oxidized Ru^{III} with 0.2 M $[Ru(NH_3)_6]^{3+}$ as acceptor (left) and the associated transient absorption traces at 510 and 570 nm (right): (a) At pH = 3, the product is the protonated radical ($Trp^{\bullet}H^{+}$) with absorption maxima at 540−590 nm.[26] The traces at 510 and 570 nm show an initial "spike" at all pH values due to the rapid excitation and oxidative quenching of the Ru^{II} moiety. At pH = 3 the absorption then increases at both wavelengths with a time constant of ca. 60 ns, as the tryptophan is oxidized by the attached Ru^{III}; (b) At pH = 8, the initial product is the protonated radical $Trp^{\bullet}H^{+}$ (solid line, 50 ns after the flash) that deprotonates to give the $Trp^{\bullet}$ radical with an absorption maximum at 520 nm[26] (line with points, 500 ns after the flash). The deprotonation time constant for $Trp^{\bullet}H^{+}$ was $\tau \approx 130$ ns, as determined from the decay trace at 570 nm and the concomitant rise at 510 nm; (c) At pH = 12, most of the initial product is already the deprotonated radical $Trp^{\bullet}$. Only a fraction of the tryptophan shows a rapid signal decay ($\tau \approx 40$ ns) at 570 nm due to deprotonation (see text).

around 400 and 600 nm and the bleach of the Ru^{II} ground state around 450 nm (Figure 2).[25] The intramolecular PCET (eq 2) could then be followed using the subsequent transient absorption changes: the Ru^{II} absorption recovery at 450 nm and the generation of the $Tyr^{\bullet}$ radical at 400 nm or the $Trp^{\bullet}$ radical around 510 nm (Figures 2 and 3).

$$[Ru^{III}-TyrH]^{3+} \rightarrow [Ru^{II}-Tyr^{\bullet}]^{2+} + H^{+} \qquad (2a)$$

$$[Ru^{III}-TrpH]^{3+} \rightarrow [Ru^{II}-Trp^{\bullet}]^{2+} + H^{+} \qquad (2b)$$

During the PCET process, which was completed within 15 μs, the $MV^{\bullet+}$ signal at 600 nm remained unchanged (Figure 2),

(19) Dixon, W. T.; Murphy, D. *J. Chem. Soc., Faraday Trans.* **1976**, *72*, 1221.
(20) (a) Nguyen, N. T.; Wrona, M. Z.; Dryhurst, G. *J. Electroanal. Chem. Int. Electrochem.* **1986**, *199*, 101. (b) Tucker, D. J.; Bond, A. M.; Qing, Z.; Rivett, D. E. *J. Electroanal. Chem. Int. Electrochem.* **1989**, *261*, 127.
(21) In ref 17b a somewhat lower value of 3.7 was given, but the exact value is not critical for the present paper.
(22) Remers, W. A.; Brown, R. K. *Indoles, Part 1. (Chemistry of Heterocyclic Compounds 25)*; Houlihan, W. J., Ed.; Wiley: New York, 1974.

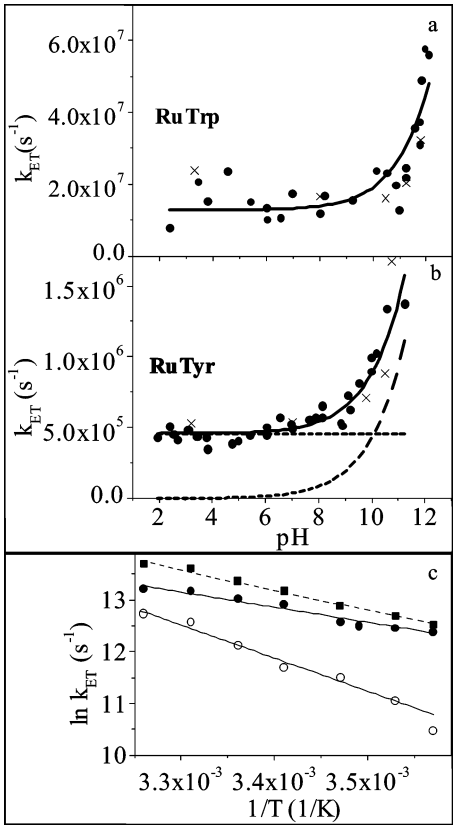

Figure 4. pH-dependence of the rate constant for electron transfer from tryptophan or tyrosine to the flash-quench generated Ru^{III} in (a) **Ru-Trp** and (b) **Ru-Tyr**. The solid line is a fit of the data to a sum of one pH-dependent and one pH-independent term, shown as dashed lines. The former term follows eqs 3−4 and is due to the CEP mechanism, while the latter term is due to the pH-independent ETPT mechanism. The dots and crosses are data in 20 and 2 mM phosphate/borate (1:1) buffer, respectively. (c) The temperature-dependence of the rate constant for **Ru-Tyr** at pH = 2.7 (solid circles) and at pH = 8.8 (squares). The data extracted for CEP at pH = 8.8 is shown as open circles. Conditions: 50 μM **Ru-Trp** or **Ru-Tyr** and 0.2 M methyl viologen dichloride.

showing that recombination with the reduced acceptor did not interfere with the PCET process. Observation of the spectra for the amino acid radical species was facilitated by the use of the hexammineruthenium(III) acceptor instead of MV^{2+}, which itself gave no significant absorption change when reduced (Figures 2 and 3).

The PCET reaction was studied at different pH values, which proved to give information about the different reaction mechanisms. The PCET driving force is pH-dependent because a proton is released to bulk water. It is determined by the difference between the electrochemical potential for the $Ru^{III/II}$ oxidant and the $Tyr^{\bullet}$/Tyr or $Trp^{\bullet}$/Trp couples (see above, Figure 1). The pH-dependence of the first-order rate constant for PCET in **Ru-Trp** and **Ru-Tyr** is shown in Figure 4. Interestingly, it does not mirror the pH-dependence of the driving force. This is in contrast to the results for our previously reported $Ru\text{-}Tyr_{ref}$.[10] Instead the rate for both **Ru-Tyr** and **Ru-Trp** remains constant over a large pH range where the driving force is pH-dependent, and becomes pH-dependent only at higher pH values.

Starting the discussion with **Ru-Trp**, the driving force is small ($\Delta G° = -0.16$ eV) at pH < 4.7 because the oxidized tryptophan is not deprotonated ($pK_a = 4.7$). The reaction is then obviously a pure electron transfer (ET), and a pH-independent rate is observed. At pH > 4.7 the driving force increases with pH, because the ET is now coupled to deprotonation of the tryptophan radical (PCET). The rate, however, remains constant up to pH ≈ 9 (Figure 4a). At pH > 9 instead the rate is strongly pH-dependent. This behavior can be explained by a switch of the PCET reaction mechanism.

The transient spectra and kinetic traces of Figure 3 give evidence that a switch indeed does occur. At pH < 4.7, the broad absorption in the range 520−600 nm is typical for $TrpH^{\bullet+}$[26] and shows that the oxidized tryptophan remains protonated (Figure 3a), as expected for a pure ET below the pK_a value. The traces at 510 and 570 nm show an instantaneous absorption from the Ru^{II} excited state that decays rapidly as this is oxidatively quenched by $Ru(NH_3)_6^{3+}$. These two processes result in the initial "spike" of the traces presented in Figure 3. Then the absorption at both wavelengths increases again with a time constant of ca. 60 ns, as the $TrpH^{\bullet+}$ radical is formed in the pure ET reaction: $Ru^{III}-TrpH \rightarrow Ru^{II}-TrpH^{\bullet+}$. At pH > 4.7, the ultimate product is instead the deprotonated tryptophan radical. In the pH region from 4.7 to ca. 9, however, our transient spectra (Figure 3b) clearly show that the initial product is the protonated radical, which deprotonates in a separate, secondary step to give the more narrow $Trp^{\bullet}$ spectrum with a maximum around 520 nm[26]: $Ru-Trp^{\bullet}H^{+} \rightarrow Ru-Trp^{\bullet} + H^{+}$. The trace at 570 nm (Figure 3b) shows an absorption decay as deprotonation occurs, with a time constant of ca. 130 ns. At 510 nm there is a small, corresponding absorption increase due to the somewhat higher absorption of the deprotonated radical. The dominating PCET mechanism in this pH range is obviously a stepwise mechanism, where electron transfer is followed by proton transfer (ETPT) to the aqueous solution. The driving force for the ET step is independent of pH (Figure 1), and the observed tryptophan oxidation rate is consequently pH-independent and equal to the rate for the pure ET reaction at pH < 4.7. Finally, at pH > 10, where the rate constant is pH-dependent, the transient spectra show that most of the initial product is already the deprotonated $Trp^{\bullet}$ radical (Figure 3c). This is indeed consistent with a switch to a concerted electron transfer−deprotonation (CEP) mechanism at high pH. The transient absorption traces at 570 nm show that a fraction of the tryptophan still deprotonates after oxidation and thus reacts via ETPT. This fraction is ca. one-third at pH = 12, as determined by a comparison of the amplitudes of the 570 nm traces in Figure 3b and 3c. This is in good agreement with what is expected from the relative rates for ETPT and CEP at this pH. The deprotonation at pH = 12 is somewhat faster ($\tau \approx 40$ ns)[27] than at pH = 8, presumably because of the high concentration of OH^- or buffer anions that may be the primary proton acceptor for the $TrpH^{\bullet+}$ radical at high pH values in the ETPT reaction. The fact that the PT step is slow enough also at pH = 12, so that the two steps of ETPT can be followed and resolved in a fraction of the complexes, proves that the main part of the complexes must undergo a different reaction

(23) Hercules, D. M.; Lytle, F. E. *Photochem. Photobiol.* **1971**, *13*, 123.
(24) Chang, I. J.; Gray, H. B.; Winkler, J. R. *J. Am. Chem. Soc.* **1991**, *113*, 7056.
(25) Kalyanasundaram, K. *Photochemistry of Polypyridine and Porphyrine Complexes*; Academic Press: London, 1992.
(26) Solar, S.; Getoff, N.; Surdhar, P. S.; Armstrong, D. A.; Singh, A. *J. Phys. Chem.* **1991**, *95*, 3636.
(27) A value from a single exponential fit at 570 nm. As the transient absorption changes from the deprotonation are convolved with those from the only somewhat faster initial oxidation, this is probably an upper limit of the time constant.

mechanism, which is CEP. Note that the observed generation of Trp• radical is not simply limited by the initial photo-oxidation of the ruthenium, as shown by the fact that the ruthenium emission decay kinetics is faster and the fact that the rate constant for Trp• generation increases monotonically with pH without leveling out (Figure 4a). To conclude, it seems clear that the dominating reaction mechanism switches from a stepwise ETPT at low pH to a concerted electron transfer−deprotonation (CEP) mechanism at high pH.

In **Ru-Tyr** the rate constant follows a pH-dependence very similar to that for **Ru-Trp** (compare Figure 4b and 4a). The scatter of the data is smaller than that for **Ru-Trp** simply because the yield of Ru^{III} was higher, resulting in larger signals. Because the pK_a of the tyrosine radical is −2, the ultimate product at all pH values examined is the deprotonated Tyr•. As for **Ru-Trp** the pH-independent region at low pH can be explained by an ETPT mechanism, in which the rate-determining step is the initial, pH-independent ET. Because of the very low pK_a value of the oxidized tyrosine, the subsequent deprotonation is much faster than the initial ET and the Tyr•H$^+$ intermediate cannot be detected. The transient absorption spectra of Figure 2 show the initial bleach of the $Ru^{II}(bpy)_3$ absorption around 450 nm due to the formation of Ru^{III}. Note that reduction of the $[Ru(NH_3)_6]^{3+}$ acceptor does not contribute to detectable absorption changes in the wavelength range shown. The subsequent 450-nm bleach recovery is accompanied by a rise of the Tyr• absorption: a characteristic double peak around 400 nm and a weaker, broad band around 600−750 nm.[28] A persistent fraction (ca. 3%) of 450 nm bleach was attributed to a ruthenium impurity without active tyrosine. Subtraction of 3% of the initial bleach from the spectrum at 7.8 μs gave the pure Tyr• spectrum (Figure 3c, inset). At pH above ∼8 the rate becomes strongly pH-dependent, and we attribute this to a switch to a CEP, as for **Ru-Trp**. Note that the behavior of **Ru-Tyr** is in sharp contrast to our results for the previously reported Ru−Tyr_{ref} complex that displayed a pH-dependent rate of PCET in the whole range investigated (5 < pH < 10).[10] Note also that the pH-dependence shown in Figure 4 does not arise from involvement of the tyrosinate anion. Instead, the tyrosine oxidation kinetics at pH around the tyrosine pK_a is biexponential, because the significant fraction of tyrosinate present already before the flash at pH > 9 reacts very rapidly by pure ET to Ru^{III} (τ < 10 ns, limited by the initial Ru^{III} generation; not shown). Only the rate constant for PCET of the phenol form is plotted in Figure 4. The amplitude of this kinetic component decreases as pH increases around the pK_a of tyrosine, as more of the tyrosine is in the phenolate form.

The kinetic deuterium isotope effect displays additional differences between the ETPT and CEP mechanisms. In experiments on **Ru-Tyr** performed in D_2O, exchanging the phenolic tyrosine proton, the observed rate constant is pH-independent with a rate constant $k_D \approx 2.5 \times 10^5$ s^{-1} in the whole range examined (2 < pH < 11, not shown), showing that CEP can never compete with ETPT in this case. This gives a limiting value of $k_H/k_D > 10$ for CEP, while the effect on ETPT is more modest: $k_H/k_D = 2$.

The temperature dependence of the PCET rate constant in **Ru-Tyr** (Figure 4c) gave further important mechanistic information. At pH = 2.7 the CEP contribution is negligible and the observed temperature dependence is that of the ETPT reaction. At pH = 8.8 instead, when the CEP contribution is significant, the temperature dependence is much stronger. Importantly, this shows that the activation energy for the concerted reaction is much higher, despite a greater driving force compared to that for the rate-determining ET step of ETPT. The temperature-dependence for PCET in **Ru-Trp** (not shown) shows a larger scatter and uncertainty in activation energy, thus precluding a similar comparison for this complex. The same is true for the deuterium isotope effect.

It is important to make clear that the pH-dependence of the PCET reaction at high pH values cannot be explained by an initial, pH-dependent deprotonation by OH^- or the base forms of the buffers, followed by electron transfer from the amino acid anions (PTET). With a pK_a value of ca. 10, tyrosine will deprotonate very slowly ($k \approx 10$ s^{-1})[10] with H_2O as proton acceptor, and this cannot account for the observed rates. Deprotonation with OH^- as the primary proton acceptor instead gives an expected upper limit given by the pseudo-first-order rate constant for diffusional encounter, $k \leq 1 \times 10^{10}[OH^-]$ s^{-1}. At pH < 9 this would be $k < 1 \times 10^5$ s^{-1}, which is much smaller than the observed values; at, e.g., pH = 7 the predicted deprotonation rate constant would be only $k \leq 1 \times 10^3$ s^{-1}. Instead, the observed value for Ru−Tyr_{ref} is $k = 5 \times 10^4$ s^{-1},[10] and the pH-dependent part for **Ru-Tyr** follows the same dependence as Ru−Tyr_{ref}. Moreover since the concentration of OH^- increases by a factor of 10 for each pH unit, a PTET mechanism would give a much steeper pH-dependence for PCET than the one observed for any of the complexes **Ru-Tyr**, **Ru-Trp**, and Ru−Tyr_{ref}. Further important evidence, showing that a diffusion-controlled PTET mechanism cannot explain the results even at pH > 9, is provided by the kinetic isotope effect (see above). The diffusion rate and the concentration of OH^- and OD^- should be very similar in experiments with H_2O and D_2O, respectively. Instead, the observed value of k_H/k_D was as large as >10 for the pH-dependent reaction at high pH, which is clearly inconsistent with a PTET reaction. Finally, the only buffer species that would be consistent at a pH-dependence above pH = 9 is PO_4^{3-}. With 2 mM buffer (1:1 phosphate/borate) the concentration of PO_4^{3-} is the same and follows the same pH-dependence as that of OH^- at pH < 11. Thus, the arguments against PTET with PO_4^{3-} as proton acceptor are the same as those against OH^-. Separate experiments were also performed to exclude the possibility that the observed pH-dependence of the rate was due to the buffer. The rate constant obtained in 2 mM buffer solution (Figure 4, crosses) are the same as those obtained in 20 mM buffer, within the experimental uncertainty, for both **Ru-Tyr** and **Ru-Trp**. This shows that the pH-dependence and the mechanistic switch are not caused by the buffer. Similarly, for Ru−Tyr_{ref} that displayed only the pH-dependent CEP mechanism, the PCET spanned the same range of time constants in 10 mM buffer (200−2 μs in the pH interval 5−10) as in neat water.[15b] Although the pH value of an unbuffered solution is difficult to determine with precision, the important result was that the same range of time constants was reproduced, showing that the pH-dependence is not simply induced by the buffer. Note again that the CEP

(28) (a) Altwicker, E. R. *Chem. Rev.* **1967**, *67*, 475. (b) Kajii, Y.; Fujita, M.; Hiratsuka, H.; Obi, K.; Mori, Y.; Tanaka, I. *J. Phys. Chem.* **1987**, *91*, 2791. (c) Maki, T.; Araki, Y.; Ishida, Y.; Onomura, O.; Matsumura, Y. *J. Am. Chem. Soc.* **2001**, *123*, 3371.

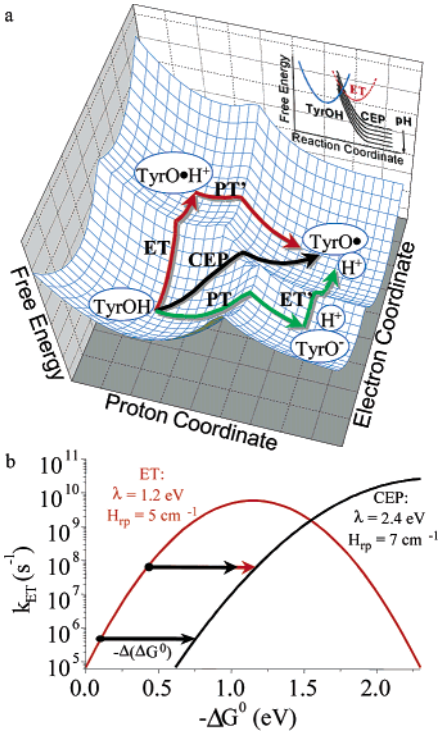

Figure 5. (a) Schematic free-energy landscape for proton-coupled electron transfer (PCET) from tyrosine (or tryptophan), used to explain our data. The two-dimensional reaction coordinate separates the nuclear motions associated with electron transfer and deprotonation. For clarity only, the surface for the lowest state at each point is shown, although the ET and PCET reactions are presumably nonadiabatic. (b) Marcus-type free energy dependence of the rate constant for ET and CEP in **Ru-Tyr** (see text). Values for λ and H_{rp} in eqs 3−4 were obtained from the fit to the data in Figure 4c.

reaction in **Ru-Tyr** follows exactly the same pH-dependence as the one in Ru−Tyr_{ref}.

CEP Reaction Model. The dependence of the rate constant on pH and temperature for PCET in **Ru-Trp** and **Ru-Tyr** can be accounted for by the mechanistic model schematically illustrated in Figure 5a. In this free-energy landscape the reaction coordinate is separated into the contributions from nuclear motions associated with electron transfer on one hand and those associated with deprotonation on the other. For a CEP reaction electron transfer and deprotonation occur as a single reaction step, with a common transition state, to directly give the deprotonated radical product. In Figure 5a this means that the reactants in the lower left corner cross the barrier (nonadiabatically) directly to the product state in the top right corner (CEP; red arrow). This gives additional reorganization energy along the proton reaction coordinate, due to the nuclear rearrangements in the transition state associated with the deprotonation (solvent polarization and internal reorganization of the phenolic group). Alternatively, they can react in a stepwise mechanism by first crossing the barrier to the protonated tyrosine radical state in the top left corner (electron transfer), followed by deprotonation (ETPT; black arrow), or vice versa (PTET; green arrow). The barrier height, i.e., the activation free energy, is distinctly different for each reaction pathway, and this is the main factor that controls the competition between the mechanisms (see below). The free energy of the product state decreases with increasing pH, because the proton released to bulk water gives the pH-dependent tyrosine potential shown in Figure 1b. This decreases the barrier for the CEP mechanism and explains the pH-dependence of the rate constant (Figure 4 at high pH). In contrast, the barrier for the pure ET step is pH-independent. At high enough pH, the barrier for CEP will be lower than that for the rate-determining ET in the ETPT mechanism, as illustrated in the inset of Figure 5a.

The driving force ($-\Delta G^{\circ\prime}$) increases with pH as given by the redox data in Figure 1, because the proton is released to bulk water. We found for the Ru−Tyr_{ref} complex[10] that the CEP rate constant as a function of pH can be fitted to a Marcus equation for electron transfer[6] (curved dashed line in Figure 4b):

$$k = A \exp\left(-\frac{(\Delta G^{\circ\prime} + \lambda)^2}{4\lambda RT}\right) \quad (3a)$$

$$A = \frac{2\pi}{\hbar}\frac{H_{rp}{}^2}{\sqrt{4\pi\lambda RT}} \quad (3b)$$

$$\Delta G^{\circ\prime}{}_{CEP} = -0.05 - 0.059 \times (\mathrm{pH} + 2)\ \mathrm{eV}\ (\textbf{Ru-Tyr}) \quad (4a)$$

$$\Delta G^{\circ\prime}{}_{CEP} = -0.11 - 0.059 \times (\mathrm{pH} - 4.7)\ \mathrm{eV}\ (\textbf{Ru-Trp}) \quad (4b)$$

where the reorganization energy λ determined from the temperature-dependent data (see below) is the energy required to reorganize the nuclear coordinates and H_{rp} is the electronic coupling between the reactant and product states. Also the pH-dependent data for **Ru-Tyr** and **Ru-Trp** could be fitted to eqs 3−4. The solid lines in Figure 4a,b are the sum of a pH-dependent CEP rate constant that follows eqs 3−4 and a pH-independent rate constant for ETPT. For **Ru-Tyr** the reorganization energy was fixed to the value determined from the temperature-dependent data (see below).

It is very interesting that the rate of CEP follows the pH-dependence given by eqs 3−4, because the pH-dependence of $-\Delta G^{\circ\prime}$ has an entirely entropic origin, in the mixing entropy of the released proton. This behavior, reported here and in our previous paper,[10] has to the best of our knowledge, not been reported before for PCET, and it has even been argued[29] on theoretical grounds that the rate of CEP cannot be pH-dependent. The result is also in sharp contrast to that of a pure deprotonation of simple acids. The latter shows no rate dependence on pH before OH^- becomes the dominating proton acceptor at high pH, after which the rate increases 10-fold per pH unit,[30] i.e., very differently from the presently shown pH-dependence. In order for the CEP to follow eqs 3−4, it cannot be governed by a single proton acceptor molecule or a small cluster of water molecules (as for a pure deprotonation[30]) but by the proton activity that is a property of a large ensemble of water molecules. This does not necessarily imply that the proton moves a large distance in the primary step of CEP. Instead, it may be conceivable that each reactant and its immediate vicinity sample a representative number of solvent microconfigurations on the reaction time scale to correctly reflect the mixing entropy of the proton at the given pH, so that all react with a single rate constant as given by eqs 3−4. The microscopic description of the pH-dependence is an important point for further theoretical and experimental investigation.

(29) Krishtalik, L. I. *Biochim. Biophys. Acta* **2003**, *1604*, 13.
(30) (a) Eigen, M. *Angew. Chem., Int. Ed. Engl.* **1964**, *3*, 1. (b) Gutman, M.; Nachliel, E. *Biochim. Biophys. Acta* **1990**, *1015*, 391.

Table 1. Proton-Coupled Electron Transfer (PCET) Parameters for Ru−Tyr, as Defined in Eqs 3−4

mechanism	H_{rp} (cm^{-1})	λ (eV)	$\Delta G^{\circ\prime}$ (eV)	k_H/k_D[a]
ETPT	5	1.2	−0.05	2
CEP	7	2.4	−0.58[b]	>10[c]

[a] Kinetic isotope effect (see text). [b] At pH = 7. [c] Lower limit at pH = 11.

Equation 3 holds also for the electron-transfer step of ETPT, but with a pH-independent value of $\Delta G^\circ = -0.05$ and -0.11 eV for **Ru-Tyr** and **Ru-Trp**, respectively. The rate of ETPT is controlled by the initial ET and is thus pH-independent, as observed for both complexes at low pH. The driving force for this step is smaller than that for the CEP reaction that uses all free energy available in a single reaction step. The reorganization energy (λ) in eq 3, on the other hand, is much larger for CEP than for ETPT. The temperature-dependent data for **Ru-Tyr** at pH = 2.7 (Figure 4c, solid circles) was fitted to eq 3, giving a value of $\lambda = 1.2$ for ETPT (Table 1). The data at pH = 8.8 were used to calculate a value of $\lambda = 2.4$ eV for CEP: first the ETPT contribution was subtracted from the data at pH = 8.8 (assuming the same ETPT rates as at pH = 2.7) to give the CEP rate constants (Figure 4c, open circles). Then these data are affected by the significant reaction entropy for CEP when a proton is released to water, making $\Delta G^{\circ\prime}$ temperature-dependent, which contributed to the larger slope of the CEP data. To correct for this, $\Delta G^{\circ\prime}$ was replaced by $\Delta H^{\circ\prime} - T\Delta S^{\circ\prime}$ in the fit of the temperature-dependent data to eqs 3−4, where $\Delta S^{\circ\prime}$ is essentially equal to the mixing entropy of the released protons ($T\Delta S^{\circ\prime} \approx 0.41$ eV at pH = 7; see ref 15b).

The much larger value of λ for CEP than for ETPT must be attributed to differences in the proton reaction coordinate. In a concerted reaction the phenolic O−H bond is broken, and in our model the system moves also along the proton reaction coordinate to the CEP transition state in Figure 5. Note that this coordinate should not be identified as the O−H bond length, since the proton may be viewed as a quantum mechanical particle, but is composed of polarization of the solvent and bond length changes of the phenolic group (see below). This gives an additional reorganization energy for CEP. The ET step of the ETPT mechanism involves an entirely different transition state with much smaller changes in the proton reaction coordinate. This is also consistent with the much larger kinetic isotope effects for a concerted reaction (Table 1). An important conclusion from our data in Table 1 is that the difference between CEP and ETPT lies in the exponential parameters of eq 3: ΔG° and λ. In contrast, the pre-exponential factor in our analysis, and thus the effective electronic coupling (H_{rp} in eq 2), is essentially the same for the two mechanisms.

A theoretical calculation of the Ru−Tyr_{ref} system of ref 10 was recently presented by Hammes-Schiffer and co-workers.[14] Although we agree to a large extent, there are also some differences in our conclusions. Specifically, they drew the conclusion that a poor vibrational wave function overlap for the proton between the final and initial states (a prefactor in the analogue to eq 3) was an important factor retarding CEP compared to a pure ET, in addition to a somewhat larger solvent reorganization energy for CEP. The calculated reorganization energy for CEP was higher than that for a pure ET but not as high as the value we determined from experimental data. They had already assumed, however, that there was no significant inner reorganization associated with the proton reaction coordinate. In our model instead, the proton reaction coordinate has contributions from both solvent polarization and inner reorganization. The latter will certainly involve significant changes in bond lengths of the phenol group upon oxidation. For example, Wheeler and co-workers[31] calculated significant bond length differences between phenol and phenoxy radical (0.13 Å difference in the C−O bond, and significant changes in some of the carbon−carbon distances). The vibrational data included gave a force constant of ca. 1000 N m^{-1} for that bond, which with the bond length changes suggest an inner reorganization energy contribution for CEP as large as several tenths of an eV. There may also be contributions from reorganizations of the phenol−water proton-accepting complex. In addition, we think it is unlikely that the proton would tunnel without significant fluctuations of the distance between the heavier oxygen nuclei between which it is bound. Fluctuations that reduce the proton tunneling distance would greatly enhance the vibrational overlap. Similar considerations have been made for pure proton-transfer reactions by Hynes and co-workers[32] who included a very strong, exponential dependence of the proton coupling on the H-bond length. For the CEP reaction discussed here this contribution would appear as a temperature-dependent exponential factor of the prefactor of eq 3, which would add to the observed activation energy. Although we cannot disentangle these different contributions to our present data, we believe that our semiclassical Marcus-type analysis is a good starting point for this type of CEP reaction, which captures the experimentally observed pH-dependence and large activation energy. In the next section we show that the larger reorganization energy for CEP can in fact explain the switch of mechanism between CEP and ETPT and why ETPT is observed in **Ru-Tyr** but not in Ru−Tyr_{ref}.

Parameters That Control the Switch between CEP and ETPT. The extra driving force for CEP, due to the concerted proton release, compared to the rate determining ET step of ETPT, is $-\Delta(\Delta G^{\circ\prime}) = -(\Delta G^{\circ\prime}_{CEP} - \Delta G^{\circ\prime}_{ET})$ (Figure 1). At low pH values $-\Delta(\Delta G^{\circ\prime})$ is too small to compensate for the larger reorganization energy. Thus, the pH-independent ETPT dominates at low pH. At high pH instead $-\Delta(\Delta G^{\circ\prime})$ is larger and CEP is the fastest mechanism. In **Ru-Tyr** the mechanistic switch occurs at pH = 10 where the rates of the two mechanisms are equal (the crossing point for the dashed lines in Figure 4b). The data in Table 1 obtained from the temperature-dependent measurements independently determine a very similar value: pH = 9.5. At pH = 10 one obtains $-\Delta(\Delta G^{\circ\prime}) = 0.76$ eV. Still the ETPT can compete because of the lower reorganization energy associated with a pure ET reaction. For **Ru-Trp**, Figure 4a suggests that the switch of mechanism occurs at pH ≈ 11, underscoring that the pH at which the switch occurs is not just simply given by the pK_a value of the amino acid. For the previous Ru−Tyr_{ref} complex in ref 10 the CEP mechanism dominated at all pH values because of the lower potential of the Ru^{III} oxidant. A change in driving force has a larger effect on ETPT than on CEP. This is due to the parabolic nature of the free energy dependence (ln k vs $-\Delta G^\circ$), which makes a reaction with lower reorganization energy (ETPT) exhibit a steeper rate-dependence in the so-called Marcus normal region

(31) Qin, Y.; Wheeler, R. A. *J. Am. Chem. Soc.* **1995**, *117*, 6083.
(32) Borgis, D.; Lee, S.; Hynes, J. T. *Chem. Phys. Lett.* **1989**, *162*, 19.

(when $-\Delta G^\circ < \lambda$; see Figure 5b). The larger driving force for CEP is counteracted by a larger reorganization energy. The lower arrow shows the situation for **Ru-Tyr** at pH = 10. The extra driving force for CEP ($-\Delta(\Delta G^{\circ\prime})$, lower black arrow) gives exactly equal rate constants for CEP and ETPT. With a stronger Ru^{III} oxidant, the driving force for CEP and ETPT are increased by equal amounts. The start of the upper black arrow gives the ETPT rate for an arbitrary increase in driving force. With the same $-\Delta(\Delta G^{\circ\prime})$ as that in the first case (equal lengths of the arrows), the CEP reaction does no longer reach the same rate. Because of the steeper dependence of the rate on ΔG° for ETPT, CEP is not competitive in this case, unless $-\Delta(\Delta G^{\circ\prime})$ is further increased (red arrow). With a weaker oxidant than that in **Ru-Tyr** instead, the effect would be opposite: CEP may dominate even at moderate pH values, as was observed before for $Ru-Tyr_{ref}$.[10] This shows why the concerted CEP mechanism is "energy conservative" and may prevail in the case of weak oxidants despite the large reorganization energy. Our results will be useful for analyzing data for PCET in natural[1−5] and artificial[33] radical proteins and in model complexes.

Acknowledgment. We thank Prof. Björn Åkermark for discussions. This work was supported by The Swedish Energy Agency, The Wallenberg Foundation, The Swedish Foundation for Strategic Research, The Royal Swedish Academy of Sciences, and The Swedish Research Council.

Supporting Information Available: Electrochemical data for **Ru-Trp**. This material is available free of charge via the Internet at http://pubs.acs.org.

JA044395O

(33) (a) DiBilio A. J.; Crane, B. R.; Wehbi, W. A.; Kiser, C. N. Abu-Omar, M. M.; Carlos, R. M.; Richards, J. H.; Winkler, J. R.; Gray, H. B. *J. Am. Chem. Soc.* **2001**, *123*, 3181. (b) Dai, Q.-H.; Tommos, C.; Fuentes, E. J.; Blomberg, M. R. A.; Dutton, P. L.; Wand, A. J. *J. Am. Chem. Soc.* **2002**, *124*, 10952.